Journal of Membrane Science 430 (2013) 106–112

Contents lists available at SciVerse ScienceDirect

Journal of Membrane Science

journal homepage: www.elsevier.com/locate/memsci

The effect of block length upon structure, physical properties, and transport within a series of sulfonated poly(arylene ether sulfone)s

Yanfang Fan [a], Chris J. Cornelius [a,*], Hae-Seung Lee [b], James E. McGrath [b], Mingqiang Zhang [b], Robert Moore [b], Chad L. Staiger [c]

[a] Department of Chemical Engineering, University of Connecticut, Storrs, CT 06269, USA
[b] Department of Macromolecular Science and Engineering, Virginia Polytechnic Institute and State University, Blacksburg, VA 24061, USA
[c] Sandia National Laboratories, Albuquerque, NM 87185, USA

ARTICLE INFO

Article history:
Received 24 July 2012
Received in revised form
18 October 2012
Accepted 25 November 2012
Available online 20 December 2012

Keywords:
Block length
Copolymer
Ionomer
Raman
IR
Gas transport

ABSTRACT

The gas transport and physical properties of sulfonated poly(arylene ether sulfone) was studied as a function of sulfonated and unsulfonated block length (5k:5k, 10k:10k, and 15k:15k). Viscoelastic properties were evaluated using Dynamic Mechanical Analysis (DMA) to observe polymer relaxations and domain compatibility. A decrease in glass transition temperature T_g was observed with increasing block length. 5k:5k had a single T_g (241 °C), while micro-phase separation between 10k:10k and 15k:15k domains create two T_g's that are slightly merged (191 °C, 236 °C and 182 °C, 233 °C). Swelling measurements revealed that film dimensional changes were greater in the plane normal to the film than parallel with increasing block size. He, H_2, CO_2, and O_2 permeability decreased with increasing sulfonated block length with no interchain spacing dependence. The apparent activation energy for permeation E_p increased with gas kinetic diameter size and had a maximum value for 15k:15k. A trade-off relationship between sulfonated and unsulfonated polymer block length is linked to phase separation, water swelling, and gas permeability.

1. Introduction

Gas separation properties are highly dependent on a material's composition, structure, and morphology [1–5]. High gas permeability and selectivity (permselectivity) are two important membrane properties [6]. Permeability is the normalized molecule transport through a material, which is dependent upon the thermodynamic partitioning of species between the gas and membrane [7]. Preferential selectivity is a key parameter for achieving high product purity and recovery from a mixture of gases. Typically, polymeric materials have greater gas selectivity than porous materials due to the mechanism of transport. The processability of polymers makes it an attractive material for gas separation membranes. Although there is significant polymer membrane progress, a trade-off relationship and upper bound still exists between permeability and selectivity [8]. Increasing our understanding of gas transport at the molecular level is needed in order to improve polymer properties.

Polyimide (PI) [9] and polysulfone (PSF) [10,11] based membranes are widely used in the gas separation industry. Gas selectivity and permeability improve when the structure of PSF is modified. Mchattie et al. [1] investigated the gas transport properties of a series of PSF structures modified with different bisphenol monomers. A PSF containing bisphenol-A (PSF-A) was compared to ones containing an aryl-ether (PSF-O), a thio-ether (PSF-S), and a fluorinated group (PSF-F). The study revealed that PSF containing stiffer groups were more selective and less permeable. Aitken et al. [12] showed that PSF with unsymmetrical structures had lower gas permeability and higher selectivity than symmetric ones. Lee et al. [13] studied PSF gas permeation and mechanical property relationships when trimethylsilyl (TMS) is attached to its backbone. TMS caused a decrease in chain packing, which increased polymer chain molecular motion resulting in an increase in gas transport.

Ionomers possess tailorable properties for applications such as fuel cells, reverse osmosis, and gas separation [14–16]. Lee et al. [17,19] and Harrison et al. [18] developed a novel method for synthesizing sulfonated copolymers based upon a poly(arylene ether sulfone). These ionomers have good physical properties and have been utilized as proton exchange membranes in low temperature fuel cells [20]. Gas transport is expected to be dependent upon block length and ion-exchange capacity (IEC). Understanding and predicting relationships between ionomer morphology, physical properties, and gas transport are important research areas. This work investigates gas transport through a series of poly(arylene ether sulfone) films with sulfonated and

* Corresponding author. Tel.: +1 860 486 3689; fax: +1 860 486 2959.
E-mail address: ccornelius@engr.uconn.edu (C.J. Cornelius).

0376-7388/$ - see front matter © 2012 Elsevier B.V. All rights reserved.
http://dx.doi.org/10.1016/j.memsci.2012.11.069

unsulfonated block sizes of 5k:5k, 10k:10k, and 15k:15k. Gas molecules He, H_2, CO_2, and O_2 of varying kinetic diameter (KD) were used to probe the structure. The activation energy E_p to gas transport through an ionomer was determined for each gas molecule.

2. Experimental

2.1. Materials

In this study, a series of BPSH–BPS (*x*:*y*) ionomers based upon a poly(arylene ether sulfone) were synthesized using equivalent oligomer block length of *x* and *y*. BPSH–BPS represents ionomer containing sulfonated (BPSH) and unsulfonated (BPS) oligomers. This acronym uses BP for bisphenol, S for sulfone, and H for the acid form. The ionomer's degree of sulfonation (DS) is described using XX. Oligomers of phenoxide terminated BPSH-100 and hexafluorobenzene end-capped BPS-0 were reacted to produce BPSH–BPS (Fig. 1) [19]. The unsulfonated (f_{us}) and sulfonated (f_s) block volume fractions, average block molar mass, density, IEC, water swelling dimensional change (ΔL%), and water uptake are summarized in Table 1.

2.2. Membrane preparation

Solutions of 5–7 wt% BPSH–BPS in the salt form were dissolved in N-methylpyrrolidone (NMP) and cast on flat Teflon or glass substrates. The solvent was slowly removed by evaporating over a 24 h period under vacuum at 60 °C. An additional drying step at 110 °C under vacuum for 48 h was used to remove residual NMP. Solution cast films had a nominal thickness ranging from 0.020 to 0.070 mm.

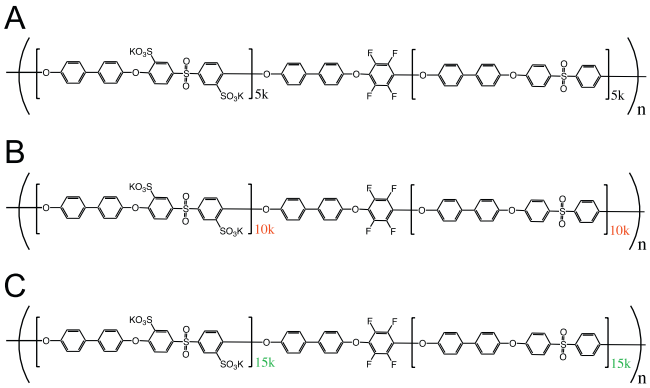

Fig. 1. Chemical structure of BPSH–BPS in K^+ form that contain equivalent amounts of sulfonated and unsulfonated blocks. (A) 5k:5k, (B) 10k:10k, and (C) 15k:15k.

Table 1
BPSH–BPS properties based upon block length.

Copolymer	Block composition f_{us}:f_s	Density (g/mL)	IEC[a] (mmol/g)	ΔL %[a] *x*:*y*:*z*	Water uptake[a] (wt%)
5k:5k	0.54:0.46	1.41	1.30	15:17:21	35
10k:10k	0.53:0.47	1.43	1.38	8:13:72	68
15k:15k	0.50:0.50	1.48	1.40	8:8:78	79

f_{us}=unsulfonated volume fraction; f_s: sulfonated volume fraction.

[a] Experimental results by Lee et al. [19,21].

2.3. Dynamic mechanical analysis

Temperature dependent mechanical behavior of BPSH–BPS was obtained using a Dynamic Mechanical Analyzer Q800 (TA instrument). Measurements were performed in the tensile mode at a frequency of 1 Hz and a temperature range from 25 °C to 250 °C. A heating rate of 2 °C/min with a strain ε_t of 0.1% was used in all tests.

2.4. Raman spectroscopy

A WITec alpha500R confocal Raman spectroscopy instrument with a Nikon 100× objective was used to confirm the IEC of BPSH–BPS. The instrument used a laser with a wavelength of 785 cm^{-1}. Data was collected using a single spectrum mode with an integration time of 10 s.

2.5. Gas transport properties

Gas species of various molecular diameters (He, H_2, CO_2, and O_2) were utilized for measuring the permeability of BPSH–BPS. A gas permeation system was custom-built in order to measure transport using the time-lag method [6,22]. The schematic diagram of the gas permeation system is shown in Fig. 2A. The permeation cell was kept at constant pressure and temperature using a convection oven (Binder Inc.). A feed pressure of 4 atm with gases having a purity of 99.99% (ultra-pure) was used to measure its transport properties. Gases were introduced into the feed side of stainless steel permeation cell, which is separated by a test film from a degassed cell of known volume at vacuum (<0.01 Torr). Increasing pressure within the low-pressure chamber is monitored as a function of time using an absolute manometer (626B, MKS Inc.).

The pressure response curve with time is divided into two regions, a steady-state and unsteady-state (Fig. 2B). Gas flux *J* is proportional to a rise in pressure (slope of P_{cell}) versus time. The flux is determined by the film's cross-sectional area A_{film}, cell volume (V_{cell}), and gas molar volume (V_m) (Eq. (1)).

$$J = slope(P_{cell})V_{cell}/(\mathrm{RT})V_m(\mathrm{STP})/A_{film} \quad (1)$$

The permeability *P* is obtained from the slope of the steady-state region and related to *J* (Eq. (2)) [6,23].In this relationship, *l* is the membrane thickness, and Δ*p* is the pressure across the film. The temperature dependence of *P* can be modeled by an Arrhenius relationship. The apparent activation energy for gas transport is E_P, P_o is the pre-exponential factor, *R* is the ideal gas constant, and *T* is temperature.

$$P = Jl/\Delta p = P_o \exp[-E_p/(\mathrm{RT})] \quad (2)$$

2.6. X-ray scattering

Wide-angle X-ray scattering (WAXS) was measured using an Oxford diffractometer with a sample-to-detector distance of 65 mm. The broad scattering peak is attributed to the average intersegmental distance between chains (*d*-space). Small angle X-ray scattering (SAXS) was obtained using a Rigaku S-Max 300 three pinhole system. The radiation source was CuKα and the incident beam was attenuated to a wavelength λ of 0.154 nm with a sample-to-detector distance of 16.0 cm. The *d*-space for both techniques was calculated using Bragg's equation: $n\lambda = 2d\sin(\theta)$.